Acidic Property of MFI-Type Gallosilicate Determined by Temperature-Programmed Desorption of Ammonia

Tetsuo Miyamoto, Naonobu Katada,* Jong-Ho Kim,† and Miki Niwa

Department of Materials Science, Faculty of Engineering, Tottori University, 4-101 Koyama-cho Minami, Tottori 680-8552, Japan

Received: October 28, 1997; In Final Form: April 16, 1998

Temperature-programmed desorption of ammonia was applied to gallosilicate with MFI structure using the water vapor treatment method to remove the unnecessary low-temperature peak and the curve-fitting method to calculate the acid strength and its distribution based on the thermodynamics. The determined acid amount approximately agreed with the [Ga]−[Na] content in the low gallium content region, showing the stoichiometric generation of one acid site by the substitution of one gallium atom, and stoichiometric neutralization of one acid site by one sodium atom. The acid strength (adsorption heat of ammonia) due to the framework gallium was ca. 130 kJ mol^{-1} with the small distribution, close to that on the ZSM-5 type aluminosilicate, and was independent of the composition. This shows that the substitution of Al and Ga into the zeolitic crystal generates the similar acid strength, and the acidic strength is mainly determined by the crystal structure. The extraframework gallium on the ion-exchange site, which was readily formed with the gallium content higher than 0.3−0.4 mol kg^{-1}, generated the additional type of acid site with the higher adsorption heat of ammonia.

Introduction

Zeolite, which consists of SiO_2 and Al_2O_3, has widely been used as a heterogeneous catalyst.[1−6] In place of the aluminum, various kinds of metals can be incorporated into the framework, and the obtained metallosilicates are being considered as novel functionalized materials.[7] Especially, gallosilicate with MFI structure has a remarkable catalytic activity for the conversion of alkane into aromatics.[8−18]

Generation of acidity by isomorphous substitution of silicon by gallium is presumed to be the origin of the catalytic functions. Analysis of the acidic property, namely, the number, strength, and nature (Brønsted or Lewis) of the acid sites, is therefore important to interpret the catalytic functions and, moreover, must be important also from the physicochemical viewpoint.

The acidic property of gallosilicate has been investigated by means of the infrared (IR) spectroscopy of surface hydroxide,[19−22] the adsorbed pyridine,[23] carbon monoxide[24,25] and nitrogen,[25] and the nuclear magnetic resonance of proton (^{1}H NMR),[26] supported by quantum chemical calculations.[27−30] These spectroscopic methods mainly deal with the quality of the acid site, but the quantitative measurement is difficult. Traditional indicator[31] and amine titration[32] methods to quantify the acid amount have a disadvantage, because they are confused by the slow diffusion of liquid molecules in the micropore. Test reactions have widely been used, but they cannot be related simply to the acidic property. Measurement of adsorption heat of such a small base as ammonia by calorimetry[33] is one powerful method to evaluate the number and strength of acid sites. By this method, the interaction between the acidic and basic materials is directly evaluated, and this gives an absolute measure of the amount and strength of acid.

Temperature-programmed desorption (TPD) of ammonia is another important method to measure the interaction between the solid acid and simple basic molecule. It is convenient for quick determination of the number and strength of acid sites on zeolite.[34−49] Also to the gallosilicate, the TPD method has been applied.[15,17,22,24,50] However, the TPD method has several problems to mislead the interpretation of acidic property in these studies.

TPD spectrum on a strongly acidic zeolite such as H-mordenite has two desorption peaks, named *l*- (lower) and *h*- (higher temperature) peaks.[34] The intensity of the *l*-peak depended on the evacuation time after ammonia had been adsorbed. The long-time evacuation at 373 K for 16 h completely removed the *l*-peak, while the *h*-peak was not affected.[51] On the Na-type zeolites, which presumably had no acidity, only the *l*-peak was observed.[52] On the other hand, the number of ammonia molecules that showed the *h*-peak generally with to the number of framework aluminum atoms in H-mordenite and H−ZSM-5,[53] or agreed with the [Al]−[Na] content when sodium was included.[52] Based on these observations, the *h*-peak was ascribed to the ammonia which had been adsorbed on the acid sites, whereas the *l*-peak was assigned to weakly held ammonia.

In the case of such a strongly acidic zeolite as mordenite, the *l*- and *h*-peaks can be separated graphically. Then we can obtain the number of acid sites from the intensity of the *h*-peak. However, the shape and position of the *h*-peak cannot be related directly with the acid strength. Because the peak position is affected by the readsorption of ammonia,[54] the calculation based on the theoretical equation is needed. We have proposed the theoretical equation on the basis of the equilibrium between the gaseous and adsorbed ammonia.[55] A method to calculate the averaged adsorption heat of ammonia from one-point experiment was proposed,[56] and then a curve-fitting method to determine the averaged adsorption heat and its distribution by simulating the TPD curve was proposed.[52] This method was

* Corresponding author. Phone +81-857-31-5684, fax +81-857-31-0881, e-mail katada@chem.tottori-u.ac.jp.

† Present address: Department of Chemical Technology, Chonnam National University, Kwangju 500-757, Korea.

S1089-5647(98)00007-8 CCC: $15.00
Published on Web 08/05/1998

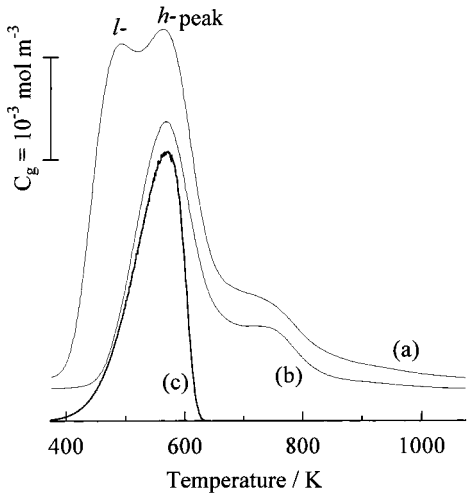

Figure 1. TPD spectrum of Na(0.12)G(0.25) before water vapor treatment (a), after water vapor treatment (b) and simulated curve (c).

applied to strongly acidic zeolites, i.e., mordenite, ZSM-5,[52] and β,[57] to clarify the acidic properties.[49,58]

However, the *l*- and *h*-peaks seriously overlap each other in the case of gallosilicate, showing such a small *h*-peak as in Figure 1a. The graphical separation is impossible in this case, and therefore the removal of the *l*-peak is necessary to measure the acidic property.

Chester et al. reported that co-feed of water vapor into the carrier gas during the TPD measurement could remove the *l*-peak.[59,60] Bagnasco reported that the feed of water vapor after the adsorption of ammonia also removed the *l*-peak.[61] From these phenomena, it is suggested that the introduced water vapor can replace the weakly held ammonia. We have improved the TPD method using this principle. The weakly held ammonia showing the *l*-peak, probably the hydrogen-bonded species, was selectively removed, while the ammonium cation bonded to the acid site, which showed the *h*-peak, was not affected. The acidic property of Y zeolite, which also showed the overlapping peaks unless this method was applied, was measured by the improved TPD method.[58,62,63]

In this paper, the acidic properties of the gallosilicate samples with various compositions were measured by the improved TPD method. The acidic property of this novel material was first determined quantitatively, and the relationship between the acidic property and composition was clarified.

Experimental Section

Synthesis of Gallosilicate. Gallosilicate was synthesized according to Argauer et al.[66] Gallium nitrate and tetra-*n*-propylammonium bromide were solved into an aqueous solution, and this was dropped slowly into a Ludox HS40 silicate solution. Sodium carbonate solution was then added. Sodium hydroxide or sulfuric acid was added to adjust the pH to 9.7. Thus mixed solution was stirred and heated at 423 K for 72 h in an autoclave. The yielded solid was filtered, washed with water, and finally calcined at 813 K for 20 h in flowing oxygen. Thus obtained Na-type gallosilicate was converted into HNa- or H-type by ion-exchange in an ammonium nitrate solution at 343 K for 24 h, followed by calcination in flowing oxygen at 813 K for 20 h. The gallium and sodium contents were measured by an inductively coupled plasma (ICP) photoemission spectrometer (Shimadzu ICPS-5000). In the following description, the gallosilicate with x and y mol kg^{-1} of the Na and Ga contents, respectively, is termed as Na(x)G(y), and the H-type with less than 0.04 mol kg^{-1} of the Na content is termed as HG(y). The contamination of aluminum was confirmed to be less than 10^{-2} mol kg^{-1}.

Impregnation of gallium on gallosilicate and silicalite was carried out in order to clarify the acidic property of extraframework gallium atoms. The gallosilicate powder was put into an aqueous solution of gallium nitrate, heated on a hot plate, dried, and calcined at 813 K for 20 h in flowing oxygen. The sample on which z mol kg^{-1} of the gallium has been loaded is termed as Ga(z)G(x).

Characterization. To show the crystal structure, powder X-ray diffraction (XRD) was recorded by a Rigaku Miniflex Plus diffractometer with 0.45 kW Cu Kα X-ray source (30 kV, 15 mA). A scanning electron microscopy (SEM) photograph was taken with a JEOL JSM-5800 scanning microscope after the deposition of thin gold film by a JEOL FINE COAT JFC-1100 ion sputter. Adsorption isotherm of nitrogen was measured at 77 K under 0.1 Pa to 90 kPa of the nitrogen pressure ($p/p^0 = 10^{-6}-0.9$). The surface area was calculated from the isotherm according to the Langmuir equation. Infrared (IR) spectrum was collected on the self-supporting disk with 10 mm of the diameter molded from 10 to 20 mg of the silicate powder in an in-situ cell by a JASCO FT/IR-5300 spectrometer.

Temperature-Programmed Desorption of Ammonia. The equipment and procedure were detailed in our review.[49] The sample (0.1 g) was set in a quartz cell and evacuated at 773 K for 1 h under <0.4 Pa of the evacuation degree. Then ammonia (13.3 kPa) was introduced into the cell, and the pressure was kept for 30 min at 373 K. After evacuation for 30 min, water vapor was introduced into the sample cell; i.e., the sample was exposed to water vapor (2−4 kPa, vapor pressure of the room temperature) at 373 K for 30 min, followed by evacuation for 30 min. For the standard experiments, the introduction of water vapor and evacuation were twice repeated, because the twice repetition of this procedure has been found to completely remove the unnecessary *l*-peak but not affect the *h*-peak on H- and Na-mordenite and Y zeolite.[58,62,63] After these treatments, the adsorbed ammonia was desorbed in helium flow (0.044 mmol s^{-1}) under ca. 13.3 kPa of the total pressure with 10 K min^{-1} of the heating rate from 373 K. The desorbed ammonia was analyzed by a mass spectrometer (ULVAC, UPM-ST-200P). Although the molecular weight of ammonia was 17, the fragment with $m/e = 16$ was used to quantify ammonia, because the parent peak with $m/e = 17$ was affected by the desorbed water.[62]

The obtained spectrum was analyzed with the curve-fitting method.[52] The TPD spectrum was simulated according to the theoretical equation expressing the desorption of ammonia

$$C_g = -\frac{\beta A_0 W}{F}\frac{d\theta}{dT} = \frac{\theta}{1-\theta}\frac{p^0}{RT}\exp\left(-\frac{\Delta H}{RT}\right)\exp\left(\frac{\Delta S}{RT}\right) \quad (1)$$

where C_g is the concentration of ammonia in gas phase (mol m^{-3}), β is the heating rate (K s^{-1}), A_0 is the desorption amount of ammonia (mol kg^{-1}), W is the sample amount (kg), F is the flow rate of carrier gas (m^3 s^{-1}), θ is the coverage, p^0 is the pressure of standard conditions (1.013×10^5 Pa), R is the gas constant (8.314 J K^{-1} mol^{-1}), T is the temperature (K), ΔH is the enthalpy change (adsorption heat of ammonia, J mol^{-1}), and ΔS (J K^{-1} mol^{-1}) is the entropy change consisting of 95 J K^{-1} mol^{-1} of the constant term and the mixing term dependent on C_g. The parameters ΔH_{avg}, the averaged value of ΔH, and σ, distribution (standard deviation) of ΔH, were adjusted to fit the simulated curve with the observed one. Thus the parameter

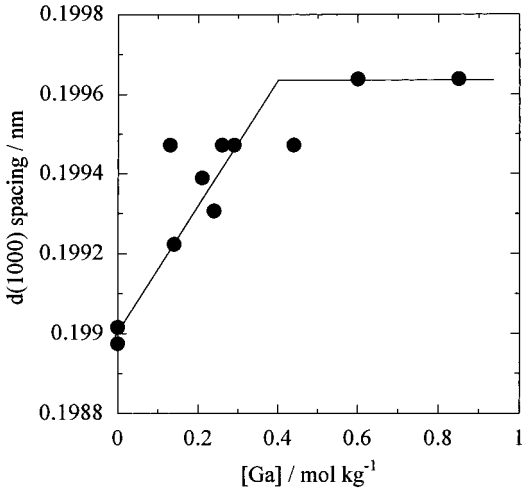

Figure 2. *d*-spacing of the (1000) plane determined from XRD over H-gallosilicate.

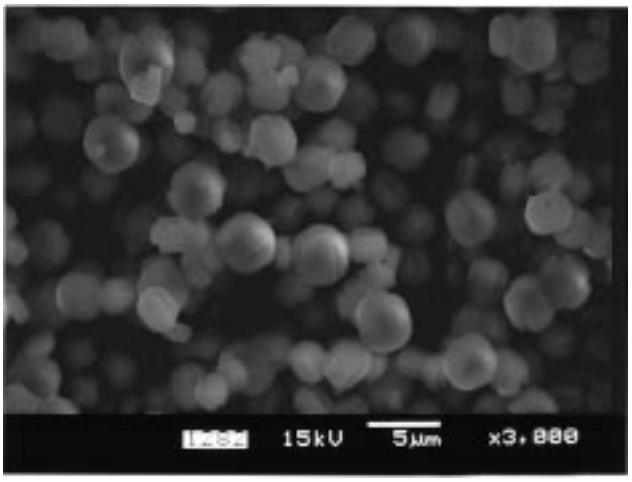

Figure 3. SEM photograph of H-gallosilicate [HG(0.26)].

set which gave the best fitted curve was selected, and this must show the acidic property of silicate.[42,52]

Results

Structure of Synthesized Gallosilicate. The X-ray diffraction (XRD) and scanning electron microscopy (SEM) measurements showed that the ion-exchange from sodium into proton and the following calcination did not affect the crystallinity and crystallite size. All the samples showed the XRD patterns ascribed to the MFI structure, and no other peak was observed. The intensity of diffraction decreased with increasing gallium content. It is known that the unit cell volume becomes larger when large gallium atoms substitute the silicon atoms in the crystal framework.[65] Figure 2 shows that the *d*-spacing increased with increasing the gallium content up to ca. 0.4 mol kg^{-1} and was unchanged by further increasing of gallium.

Figure 3 shows the typical SEM photograph of the H-gallosilicate. The crystallite shape was cylindrical, cubic, or spherical. The particle diameter was determined from the SEM images to be ca. 10 μm when no gallium was contained, and the diameter decreased with increasing gallium content. Simultaneously, the intensity of XRD decreased, as shown above, and the relationship between the intensity of (051) diffraction and the crystallite size determined from SEM is plotted in Figure 4. The XRD intensity gradually decreased with decreasing crystallite size from 10 to 1 μm, caused by increasing the gallium

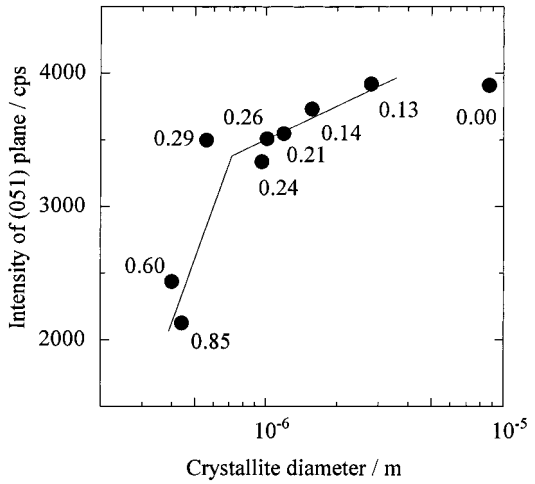

Figure 4. Plot of XRD intensity of H-gallosilicate against the crystallite size determined from SEM. The number shows the Ga content in units of mol kg^{-1}.

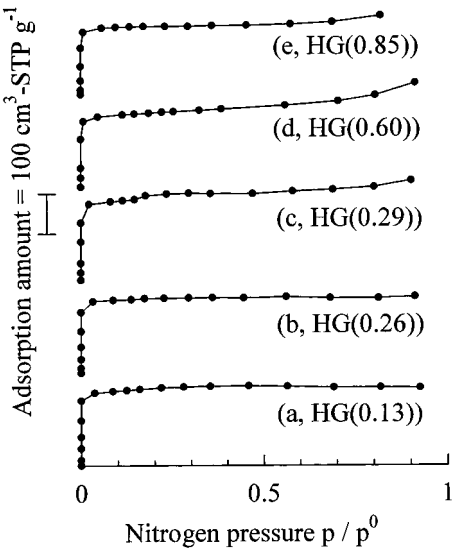

Figure 5. Adsorption isotherm of nitrogen at 77 K on H-gallosilicate [a, HG(0.13); b, HG(0.26); c, HG(0.29); d, HG(60); e, HG(0.85)].

content from 0 to ca. 0.3 mol kg^{-1}. Further increasing the gallium content significantly suppressed the XRD intensity, whereas the crystallite size slightly decreased. Generally, the XRD intensity decreases with decreasing crystallite size; even the crystallinity is maintained. The slow decrease of the XRD intensity at 0−0.3 mol kg^{-1} of the gallium content is consistent with the suppression of the crystallite size. However, the quick drop of the XRD intensity with the higher gallium content cannot be explained by only the suppression of the crystallite size. This suggests the low crystallinity induced by the high gallium content.

The adsorption isotherm of nitrogen at 77 K on gallosilicates with the gallium contents less than ca. 0.3 mol kg^{-1} was found to be I-type, as shown in Figure 5a,b, showing the microporous structure. The isotherm showed a slope at 0.5 to 1 of p/p^0 on the samples with ca. 0.3−0.8 mol kg^{-1} of gallium, as shown in Figure 5c−e, suggesting the formation of macropores (>several 10 nanometers in diameter).[68] This is probably due to the small particle size in this high gallium content range shown by the SEM. The adsorption capacity determined from the plateau of the isotherm was not related to the gallium content of less than 0.6 mol kg^{-1}, as shown by the Langmuir surface area in Figure

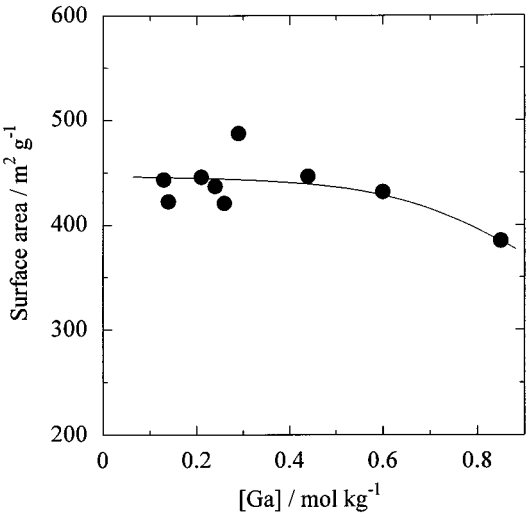

Figure 6. Langmuir surface area determined from plateau observed in adsorption isotherm of nitrogen at 77 K.

6, whereas the sample with the high gallium content (0.85 mol kg^{-1}) showed a low capacity.

Temperature-Programmed Desorption. Figure 1a shows the TPD spectrum on the gallosilicate (Na(0.12)G(0.25)) measured after the adsorption of ammonia without water vapor treatment. As observed on various zeolites,[49,52−58] the spectrum had two peaks, *l*- and *h*-peaks. Among these peaks, the *l*-peak is due to the weakly held ammonia, e.g., hydrogen-bonded one, and not related with the acidic property. The *h*-peak is ascribed to the ammonia or ammonium cation adsorbed on the acid site and must show the acidic property. Probably because this sample has a large amount of sodium,[52] the *l*-peak was so large that these peaks seriously overlapped each other. It is therefore difficult to analyze the area, position, and shape of the *h*-peak. Figure 1b shows the TPD spectrum measured after the water vapor treatment; i.e., the gallosilicate which had been adsorbed ammonia was exposed to ca. 3 kPa of water vapor. The simple *h*-peak was obtained, and it could be fitted with the curve simulated according to the theoretical eq c. Therefore, it is concluded that the water vapor treatment selectively removed the *l*-peak due to hydrogen-bonded ammonia, while the *h*-peak showing the acidic property of silicate was maintained, as observed on mordenite, Y[58,62,63] and β[57,62]-type zeolites. However, it is noteworthy that an additional peak was observed at ca. 750 K as a shoulder of the *h*-peak in both spectra before and after the water vapor treatment.

The TPD spectra were recorded with the water vapor treatment method over the gallosilicates with various Ga contents as shown in Figure 7. The silicalite with no gallium showed no desorption peak a. In all the spectra on gallosilicates (b−j), the peak maximum was observed at 550−600 K, and the peak shoulder appeared at 700−900 K. The peak shoulder was rather small in the low gallium content region (<0.3 mol kg^{-1}, (b−g), and became large in the higher gallium content region (h−j), where the *d*-spacing did not increase with increasing gallium content as shown in Figure 2. From these findings, it is suggested that the framework gallium atoms generate the acid sites showing the simple peak at 550−600 K, whereas the extraframework gallium cations and/or the Ga_2O_3 particle loaded on the silicate form the acid sites showing the additional peaks at 700−900 K. On the samples with gallium more than 0.3 mol kg^{-1}, one more additional peak shoulder was observed at ca. 450 K, and therefore the influence of the extraframework species is supposed, but this seems small.

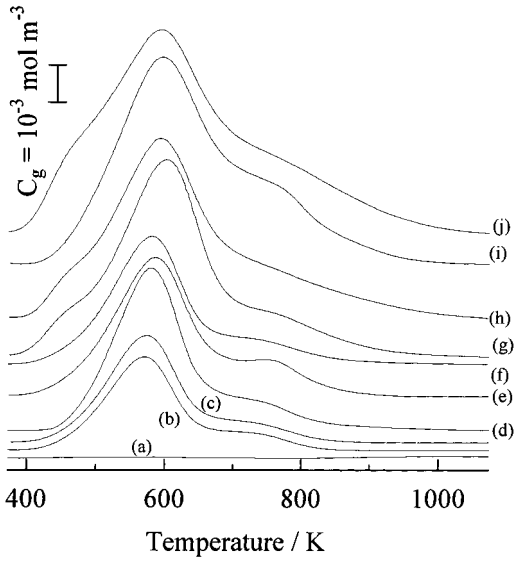

Figure 7. TPD spectra observed silicalite (a) and H-gallosilicate [b, HG(0.13); c, HG(0.17); d, HG(0.21); e, HG(0.25); f, HG(0.26); g, HG(0.31); h, HG(0.48); i, HG(0.60); j, HG(0.81)] after water vapor treatment.

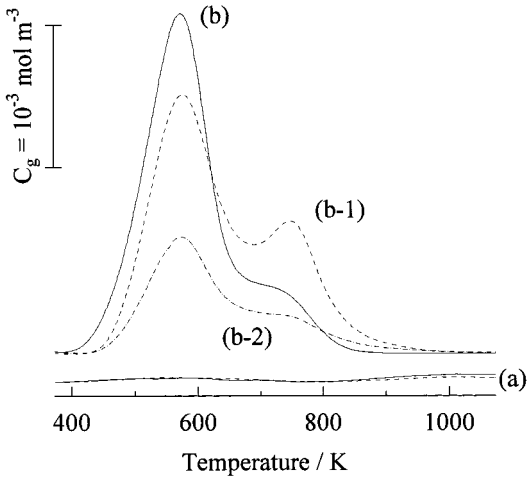

Figure 8. TPD spectra of HG(0.13) (a) and the Ga-impregnated sample (b-1, Ga(0.1)G(0.13); b-2, Ga(0.3)G(0.13)).

Identification of Peaks. To demonstrate the role of the extraframework gallium species, the impregnation of gallium salt was carried out on H-gallosilicate and silicalite. The solid line in Figure 8a shows the TPD spectrum on pure silicalite, demonstrating no acidity. The spectrum on the gallium-loaded sample (a, dotted line) shows no generation of acidity by the impregnation of gallium on silicalite.

On the other hand, the TPD spectrum on H-gallosilicate (b) was significantly changed by the gallium impregnation. The loading of 0.1 mol kg^{-1} of gallium made the peak at 750 K large and clear (b-1). This suggests that the extraframework gallium atom loaded on gallosilicate is the origin of the latter peak. Further loading (0.3 mol kg^{-1}, b-2) suppressed both peaks.

Figure 9a shows the infrared (IR) spectrum of the evacuated H-gallosilicate: the isolated silanol (3722 cm^{-1}), acidic hydroxide (3608 cm^{-1}), and skeletal vibration (2002, 1879, and 1637 cm^{-1}) were observed. The spectrum of the adsorbed pyridine after the evacuation at 373−573 K (Figure 9, b−d) shows the presence of a relatively large amount of Brønsted (1547 cm^{-1}) and small amount of Lewis (1458 cm^{-1}) acid sites. After the impregnation of 0.1 mol kg^{-1} of gallium, the peak

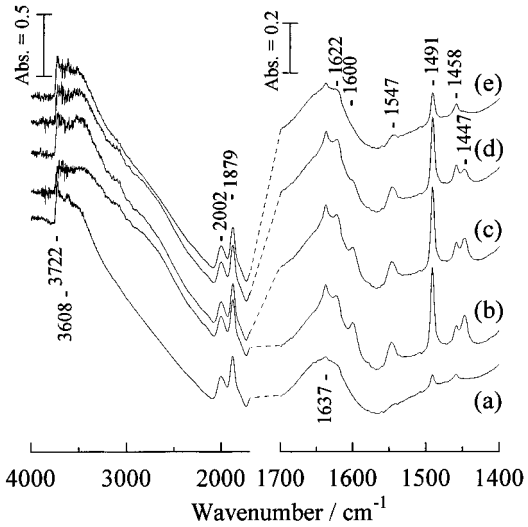

Figure 9. IR spectra of HG(0.13) evacuated at 773 K for 1 h (a), followed by the adsorption of pyridine (ca. 0.4 kPa) at 373 K for 30 min and evacuation at 373 (b), evacuation at 473 (c), 573 (d), and 673 K (e).

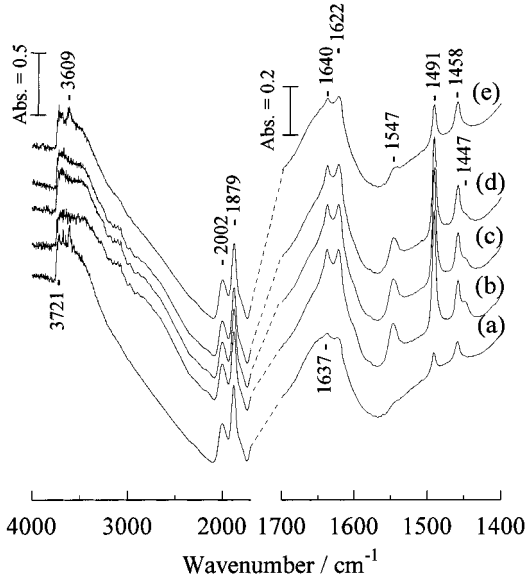

Figure 10. IR spectra of Ga(0.1)G(0.13) evacuated at 773 K for 1 h (a), followed by the adsorption of pyridine (ca. 0.4 kPa) at 373 K for 30 min and evacuation at 373 (b), 473 (c), 573 (d), and 673 K (e).

due to the Lewis acid site (1458 cm^{-1}) obviously became large, as shown in Figure 10b−d. The spectrum on the gallium-impregnated silicalite showed only the hydrogen-bonded pyridine at 1445 cm^{-1}, but neither acidic hydroxide nor Brønsted and Lewis acidic species (the spectrum is not shown).

Determined Acidic Property. From the peak area, the acid amount (desorption amount of ammonia) was calculated as shown in Figure 11. The acid amount determined from the whole peak area approximately agreed with the [Ga]−[Na] content on both H- (○) and HNa-type (△) gallosilicates.

As shown above, the major part of the peak at 550−600 K probably shows the acidic property of the framework gallium atoms. The major part was fitted well with the simulated one on all the samples. The acid amount determined from the simulation was plotted in Figure 11 (● and ▲). At the [Ga]−[Na] less than 0.3 mol kg^{-1}, thus determined acid amount was slightly smaller than that determined from the whole peak area and therefore approximately agreed with the [Ga]−[Na] content. However, because the additional peak at 700−900 K was large

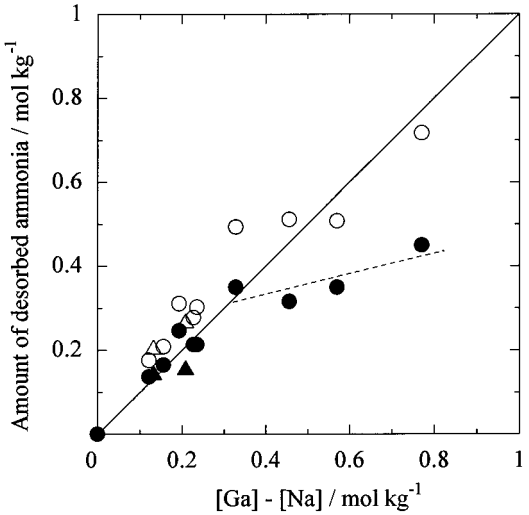

Figure 11. Plot of the acid amount determined from the whole peak area (● and ▲) and from the simulated *h*-peak (● and ▲) against [Ga]−[Na] content over H- (○ and ●) and HNa-type (△ and ▲) gallosilicate.

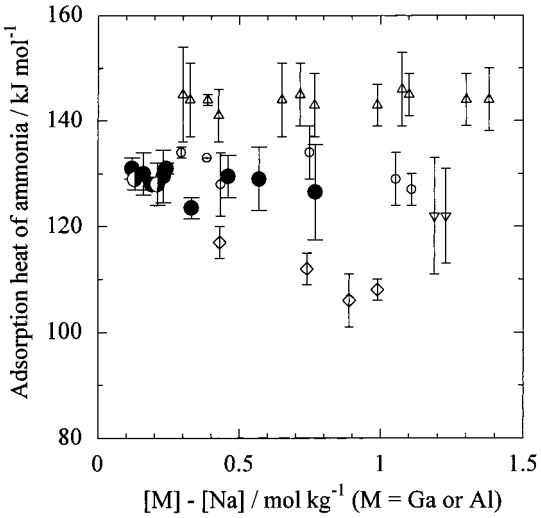

Figure 12. Averaged adsorption heat determined from the simulated *h*-peak on H- (●) and HNa- (◑) gallosilicate, mordenite (△), ZSM-5 (○), zeolite β (▽) and Y zeolite (◇). The vertical bar shows the standard deviation.

at the higher [Ga]−[Na] content as shown above, the determined acid amount was much smaller than the 1:1 relationship against the [Ga]−[Na] content higher than 0.4 mol kg^{-1}.

The acid strength (adsorption heat of ammonia) determined from the simulation was shown in Figure 12. The distribution (standard deviation) of acid strength was less than 10 kJ mol^{-1} on one silicate sample. The averaged strength on gallosilicate was almost 130 kJ mol^{-1} and hardly affected by the [Ga]−[Na] content; a variation within 10 kJ mol^{-1} was observed, but such a variation is small compared to the difference in the acid strength among the different kinds of zeolites. The difference between the H- and HNa-types, namely, the presence of sodium, did not affect the acid strength. In this figure, the acid strength of aluminosilicates determined by our previous study[52,57,58,62,63] is overlapped. On all kinds of zeolites, the acid strength distribution was small (<ca. 10 kJ mol^{-1}). The averaged acid strength was determined by the crystal structure as MOR > MFI > BEA > FAU (ca. 145, 130, 120, and 110 kJ mol^{-1}, respectively) and less affected by the composition. The similar acid strength at ca. 130 kJ mol^{-1} was thus shown on the ZSM-5 aluminosilicate and the present gallosilicate.

Discussion

Identification of Peaks. The *d*-spacing of the (1000) plane increased with increasing gallium content up to ca. 0.4 mol kg^{-1}. This shows that gallium in the parent gel was readily incorporated into the silicate crystal during the hydrothermal synthesis when the gallium content was lower than 0.4 mol kg^{-1}. In the higher gallium content region, the constant *d*-spacing indicates that the gallium more than 0.4 mol kg^{-1} was hardly incorporated into the crystal at least by the present preparation method, suggesting the presence of the extraframework gallium atoms, i.e., gallium cation located on the ion-exchange site and/or the gallium oxide particle. As shown by the SEM, the crystallite size decreased with increasing gallium content, and the formation of macropores with the gallium content higher than ca. 0.3 mol kg^{-1} shown by the nitrogen adsorption isotherm is consistent with the small crystal size. The XRD also shows the low crystallinity induced by the gallium content higher than ca. 0.3 mol kg^{-1}.

Therefore, the structural characters of the present gallosilicate samples can be summarized as follows:

1. In the gallium content region less than 0.3−0.4 mol kg^{-1}, the crystallinity was high, and gallium was predominantly incorporated into the silicate matrix.

2. In the gallium content region higher than 0.3−0.4 mol kg^{-1}, the crystallinity was low, and not a negligible amount of gallium existed outside of the framework.

In all the samples, the main peak at 550−600 K and the additional peak shoulder at 700−900 K were observed in the TPD spectrum. This was quite different from the cases of mordenite and ZSM-5 zeolites, on which the simple *h*-peak was obtained.[52] The high crystallinity, probably realized on ZSM-5 and mordenite, seems to give the stoichiometric generation of acid site and the simple acidic property. On the other hand, an additional peak or peak shoulder was observed, and the acid amount was smaller than [Al]−[Na] on β-[57] and Y-type[62,63] zeolites. The samples used for these studies possessed low crystallinities because of the difficulty of synthesis of highly crystallized β zeolite or the difficulty of ion-exchange without crystal destruction of Y zeolite. On such samples, complicated structure containing the extraframework aluminum and/or the particle of alumina and amorphous silica−alumina is suggested. Also in the present case, the extraframework gallium is suggested, especially on the samples with a high content of gallium.

In the gallium content region less than 0.3−0.4 mol kg^{-1}, the observed TPD spectrum was relatively simple, and therefore the major part of the peak at 550−600 K must show the acidic property of the acid site generated by the substitution of gallium into the MFI crystal. It is speculated that the additional peak at 700−900 K, which was relatively large in the gallium concentration region higher than 0.4 mol kg^{-1}, was due to the extraframework gallium atoms.

To confirm this speculation, the TPD spectrum on the gallium-impregnated gallosilicate was measured. As shown in Figure 8 (b-1), the impregnation of gallium generated the TPD peak at ca. 750 K. It is confirmed that the strong acid site was generated by the extraframework gallium. We have also found that the impregnation of aluminum on Al-containing ZSM-5 zeolite created the strong acidity.[67]

Because the impregnation of gallium on the pure silicalite generated no acidity (Figure 8a), this type of acid site is assumed to be generated by the copresence of the framework and extraframework gallium atoms. In other words, it is suggested that the interaction between the ion-exchange site due to the framework gallium and the extraframework gallium cation located on the ion-exchange site generated this type of acid site. The IR study (Figure 10) showed that the nature of the acid site generated by the impregnation of gallium was Lewis type.

The impregnation of a further amount of gallium suppressed both the TPD peaks at ca. 600 and 750 K (Figure 8b-2). The SEM observations showed that the impregnation of gallium formed gallium oxide particles on the external surface of silicate. Probably such an oxide particle blocked the micropores. No generation of acidity by the impregnation of gallium on the pure silicalite shown by the IR spectrum is consistent with the TPD experiments.

Determined Acidic Property. In the [Ga]−[Na] < 0.3−0.4 mol kg^{-1}, the amount of acid site due to the framework gallium atom, which was determined from the curve fitting of the major part of the peak at 550−600 K, approximately showed the 1:1 relationship against the [Ga]−[Na] content (Figure 11). This confirms the stoichiometric generation of acid site by the isomorphous-substitution of gallium atom into the silicate matrix and the stoichiometric neutralization of the acid site by sodium atom. It is noteworthy that such a complete stoichiometry has not been shown. The calorimetric study showed that the number of the strongly adsorbed ammonia approximately agreed with the gallium content,[33] but the accuracy seems lower than the present TPD method because of the difficulty in the separation of the strongly adsorbed ammonia (the species corresponding to the *h*-peak in the TPD) from the weakly held ammonia.

In the gallium content region higher than ca. 0.4 mol kg^{-1}, the acid amount due to the framework gallium, determined from the simulation of the major part of the peak, became smaller than the [Ga]−[Na] content. Previously we showed that too high an aluminum content decreased the acid amount because of the formation of the secondary-neighboring aluminum site (−Al−O−Si−O−Al-).[49,52,58] However, such a site is formed with the trivalent substituting cation more than 1.5 mol kg^{-1} on the MFI structure,[39] and therefore the relatively high amount of the extraframework gallium atoms at gallium content more than 0.4 mol kg^{-1} must be the reason for the disagreement between the framework gallium and total gallium contents.

The acid strength (Figure 12) possessed a narrow distribution within 10 kJ mol^{-1} on one sample and was close to 130 kJ mol^{-1}. A small variation in the averaged adsorption heat within 10 kJ mol^{-1} was observed, but such a variation was small compared to the difference in the acid strength among different kinds of zeolites. In this sense, the acid strength can be regarded to be independent of the composition. On zeolites, the acid strength was determined mainly by the crystal structure as MOR (ca. 140 kJ mol^{-1}) > MFI (130) > BEA (120) > FAU (110), but not by the composition,[49,52,58,62,63] as shown in Figure 12. The present study indicates that the acid strength of gallosilicate is also homogeneous, and Al and Ga substituted into the same MFI structure possess a similar acid strength. Parrillo et al. showed the similar adsorption heats of ammonia on alumino- and gallosilicates with MFI structure by means of the calorimetry.[33] The IR studies using nitrogen as a probe also proposed the similar property due to the MFI framework on Al- and Ga-MFI.[25] Density functional theory predicted that the charge on H atom, bond length, and ionicity of OH bondings of assumed $H_3Si(OH)TH_3$ cluster were changed by the substituting T atom as Al > Ga ≫ B; however, it is noteworthy that the difference in the effect between Al and Ga were quite smaller than that between Ga and B.[27] The present results, showing the similar acidic properties on alumino- and gallosilicates, support these studies.

These findings are summarized as that one gallium atom substituted into the MFI framework generates one acid site with ca. 130 kJ mol^{-1} of the adsorption heat of ammonia (acid strength), whereas the extraframework gallium on the ion-exchange site generates the additional type of acid site with the higher adsorption heat of ammonia. From the viewpoint to study the generation of acidity by isomorphous substitution, the former type of acid site is important, and the present study provides a simple conclusion that the acid strength is determined by the crystal structure but not by the composition. However, it is also noteworthy that, although the strength of the former type of acid site is not affected directly by the composition, the whole acidic property of a gallosilicate sample is affected by the composition via the formation of the latter type of acid site. This must be important to interpret the catalytic function of the gallosilicate, and indeed, the gallium-impregnated ZSM-5 has been reported to show specific functions as catalyst.[68,69] On this point, we wish to emphasize that the present TPD method, as well as the IR spectroscopy using nitrogen,[25] can distinguish between these different types of acid sites.

Conclusion

1. The number of acid sites on H-gallosilicate with MFI structure approximately agreed to the number of the gallium atoms isomorphous-substituted into the framework, and in the presence of the sodium, the number of acid sites was in agreement with the [Ga]−[Na] content. This confirms the stoichiometric generation of one acid site by the substitution of one gallium atom and the stoichiometric neutralization of one acid site by one sodium atom.

2. The acid strength (adsorption heat of ammonia) due to the framework gallium was ca. 130 kJ mol^{-1} with <10 kJ mol^{-1} of the distribution and was almost independent of the composition. This shows that the acidic strength is mainly determined by the crystal structure but less affected by the composition. This value was similar to that on the ZSM-5 type aluminosilicate, showing that the framework aluminum and gallium generate the similar acid strength. The determined strength is consistent with the previous studies using the calorimetry and the IR spectroscopy with nitrogen probe.

3. The extraframework gallium, which is readily formed with the gallium content higher than 0.3−0.4 mol kg^{-1}, generates the additional type of acid site with the higher adsorption heat of ammonia.

Acknowledgment. This study was partly supported by a Grant-in-Aid for Developmental Scientific Research from the Ministry of Education, Science, Sports and Culture, Japan (No. 06555243).

References and Notes

(1) Rabo, J. A. *Stud. Surf. Sci. Catal.* **1992**, *75*, 1.
(2) Hölderich, W. F. *Stud. Surf. Sci. Catal.* **1992**, *75*, 127.
(3) Haag, W. O. *Stud. Surf. Sci. Catal.* **1994**, *84*, 1375.
(4) Iwamoto, M. *Stud. Surf. Sci. Catal.* **1994**, *84*, 1395.
(5) Corma, A. *Chem. Rev.* **1995**, *95*, 559.
(6) Farneth, W. E.; Gorte, R. J. *Chem. Rev.* **1995**, *95*, 615.
(7) Barrer, R. M. In *Hydrothermal Chemistry of Zeolites*; Academic Press: London, 1982; p 251.
(8) Khodakov, A. Y.; Kustov, L. M.; Bondarenko, T. N.; Dergachev, A. A.; Kazanski, V. B.; Minachev, K. M.; Borbely, G.; Beyer, H. K. *Zeolites* **1990**, *10*, 603.
(9) Giannetto, G.; Montes, A.; Gnep, N. S.; Florentino, A.; Cartraud, P.; Guisnet, M. *J. Catal.* **1994**, *145*, 86.
(10) Vargas, A.; Guzman, O.; Ferrat, G.; Guzman, M. L.; *React. Kinet. Catal. Lett.* **1994**, *52*, 461.
(11) Choudhary, V. R.; Kinage, A.; Sivadinarayana, C.; Sansare, S. D.; Guisnet, M. *Catal. Lett.* **1995**, *33*, 401.
(12) Choudhary, V. R.; Kinage, A. K. *Zeolites* **1995**, *15*, 732.
(13) Choudhary, V. R.; Kinage, A. K.; Sivadinarayana, C.; Guisnet, M.; *J. Catal.* **1996**, *158*, 23.
(14) Choudhary, V. R.; Kinage, A. K.; Sivadinarayana, C.; Devadas, P.; Sansare, S. D.; Guisnet, M. *J. Catal.* **1996**, *158*, 34.
(15) Choudhary, V. R.; Sivadinarayana, C.; Kinage, A. K.; Devadas, P.; Guisnet, M. *Appl. Catal. A* **1996**, *136*, 125.
(16) Kusakabe, K.; Yokoyama, S.; Morooka, S.; Hayashi, J.; Nagata, H. *Chem. Eng. Sci.* **1996**, *51*, 3027.
(17) Choudhary, V. R.; Devadas, P.; Kinage, A. K.; Sivadinarayana, C.; Guisnet, M. *J. Catal.* **1996**, *158*, 537.
(18) Choudhary, V. R.; Devadas, P.; Sansare, S. D.; Guisnet, M. *J. Catal.* **1997**, *166*, 236.
(19) Chu, C. T.-W.; Chang, C. D. *J. Phys. Chem.* **1985**, *89*, 1569.
(20) Camblor, M. A.; Perez-Pariente, J.; Fornes, V. *Zeolites* **1992**, *12*, 280.
(21) Hedge, S. G.; Abdullah, R. A.; Bhat, R. N.; Ratnasamy, P. *Zeolites* **1992**, *12*, 951.
(22) Berndt, H.; Martin, A.; Kosslick, H.; Lücke, B. *Microporous Mater.* **1994**, *2*, 197.
(23) Yamagishi, K.; Namba, S.; Yashima, T. *Bull. Chem. Soc. Jpn.* **1991**, *64*, 949.
(24) Mirsojew, I.; Ernst, S.; Weitkamp, J.; Knözinger, H. *Catal. Lett.* **1994**, *24*, 235.
(25) Arean, C. O.; Palomino, G. T.; Geobaldo, F.; Zecchina, A. *J. Phys. Chem.* **1996**, *100*, 6678.
(26) Challoner, R.; Harris, R. K.; Barri, S. A.; Tayor, M. J. *Zeolites* **1991**, *11*, 827.
(27) O'Malley, P. J.; Dwyer, J. *Chem. Phys. Lett.* **1988**, *143*, 97.
(28) Zahradnik, R.; Hobza, P.; Wichterlova, B.; Cejka, J. *Collect. Czech. Chem. Commun.* **1993**, *58*, 2474.
(29) Langenaeker, W.; Coussement, N.; De Proft, F.; Geerlings, P. *J. Phys. Chem.* **1994**, *98*, 3010.
(30) Inui, T.; Matsuda, K. *Stud. Surf. Sci. Catal.* **1994**, *90*, 355.
(31) Hirschler, A. E. *J. Catal.* **1963**, *2*, 428.
(32) Tanabe, K. *Solid Acid and Bases*; Kodansha: Tokyo, 1970.
(33) Parrillo, D. J.; Lee, C.; Gorte, R. J.; White, D.; W. E. Farneth, W. E. *J. Phys. Chem.* **1995**, *99*, 8745.
(34) Sawa, M.; Niwa, M.; Murakami, Y. *Zeolites* **1990**, *10*, 532.
(35) Karge, H. G.; Dondur, V.; Weitkamp, J. *J. Phys. Chem.* **1991**, *95*, 283.
(36) Miller, J. T.; Hopkins, P. D.; Meyers, B. L.; Ray, G. J.; Roginski, R. T. Zajac, G. W.; Rosenbaum, N. H. *J. Catal.* **1992**, *138*, 115.
(37) Stach, H.; Janchen, J.; Jerschkewitz, H.-G.; Lohse, U.; Parlitz, B.; Zibrowius, B.; Hunger, M. *J. Phys. Chem.* **1992**, *96*, 8473.
(38) Crocker, M.; Herold, R. H. M.; Sonnemans, M. H. W.; Emeis, C. A. Wilson, A. E.; van der Moolen, J. N. *J. Phys. Chem.* **1993**, *97*, 432.
(39) Barthomeuf, D. *J. Phys. Chem.* **1993**, *97*, 10092.
(40) Kim, J.-H.; Namba, S.; Yashima, T. *Appl. Catal. A* **1993**, *100*, 27.
(41) Xu, Y.; Liu, W.; Wong, S.-T.; Wang, L.; Gao, X. *Catal. Lett.* **1996**, *40*, 207.
(42) Weber, R. W.; Fletcher, J. C. Q.; Moller, K. P.; O'Connor, C. T. *Microporous Mater.* **1996**, *7*, 15.
(43) Lezcano, M.; Ribotta, A.; Miro, E.; Lombardo, E.; Petunchi, J.; Moreaux, C.; Dereppe, J. M.; *Stud. Surf. Sci. Catal.* **1996**, *101*, 971.
(44) Choi, E.-Y.; Nam, I.-S.; Kim, Y. G. *J. Catal.* **1996**, *161*, 597.
(45) Gil, A.; Del Castillo, H. L.; Masson, J.; Court, J.; Grange, P. *J. Mol. Catal.* **1996**, *107*, 185.
(46) Kumar, N.; Lindfors, L. E.; Byggningsbacka, R. *Appl. Catal. A* **1996**, *139*, 189.
(47) Hopkins, P. D.; Miller, J. T.; Meyers, B. L.; Ray, G. J.; Roginski, R. T.; Kuehne, M. A.; Kung, H. H.; *Appl. Catal., A: General* **1996**, *136*, 29.
(48) Hunger, B.; Miessner, H.; van Szombathely, M.; Geidel, E. *J. Chem. Soc., Faraday Trans.* **1996**, *92*, 499.
(49) Niwa, M.; Katada, N. *Catal. Surveys Jpn.* **1997**, *1*, 215.
(50) Inui, T. *Stud. Surf. Sci. Catal.* **1994**, *83*, 263.
(51) Hashiguchi, T.; Sakai, S. In *Preprint of the 11th Meeting on the Reference Catalyst of Japan*; The Catalysis Society of Japan: Tokyo, 1987; p 6.
(52) Katada, N.; Igi, H.; Kim, J.-H.; Niwa, M. *J. Phys. Chem. B* **1997**, *101*, 5969.
(53) Sawa, M.; Niwa, M.; Murakami, Y. *Zeolites* **1990**, *10*, 532.
(54) Niwa, M.; Iwamoto, M.; Segawa, K. *Bull. Chem. Soc. Jpn.* **1986**, *59*, 3735.
(55) Sawa, M.; Niwa, M.; Murakami, Y. *Zeolites* **1990**, *10*, 307.
(56) Niwa, M.; Katada, N.; Sawa, M.; Murakami, Y. *J. Phys. Chem.* **1995**, *99*, 8812.
(57) Katada, N.; Iijima, S.; Igi, H.; Niwa, M. *Stud. Surf. Sci. Catal.* **1996**, *105*, 1227.

(58) Katada, N.; Igi, H.; Miyamoto, T.; Kim, J.-H.; Niwa, M. *Shokubai* (*Catalysts & Catalysis*) **1997**, *39*, 444.

(59) Chester, A. W.; Higgins, J. B.; Kuehl, G. H.; Schlenker, J. L.; Woolery, G. L. In *Preprint of the 11th Meeting on the Reference Catalyst of Japan*; The Catalysis Society of Japan: Tokyo, 1987; p 22.

(60) Woolery, G. L.; Kuehl, G. H., Timken, H. C.; Chester, A. W. In *Discussions on Zeolite and Microporous Materials: Supporting Information to the 11th International Zeolite Conference*; Chon, H., Uh, Y. S., Eds.; Hanrimwon Publishing: Seoul, 1996; p 247.

(61) Bagnasco, G. *J. Catal.* **1996**, *159*, 249.

(62) Igi, H.; Katada, N.; Niwa, M. In *Preprints of ZMPC '97*; Japan Association of Zeolites: Tokyo, 1997; p 88.

(63) Igi, H.; Katada, N.; Niwa, M. *12th Int. Zeolites Conf.* **1998**, P54.

(64) Argauer, R. J.; Landolt, G. R. U.S. Patent 3702886, 1972.

(65) Awate, S. V.; Joshi, P. N.; Shiralkar, V. P.; Kotasthane, A. N. *J. Inclusion Phenom. Mol. Recognit.* **1992**, *13*, 207.

(66) Bond, G. C. In *Heterogeneous Catalysis: Principles and Applications*, 2nd ed.; Oxford University Press: New York, 1987; p 12.

(67) Kunieda, T.; Katada, N.; Niwa, M.; *12th Int. Zeolites Conf.* **1998**, A23.

(68) Meriaudeau, P.; Naccache, C. *J. Mol. Catal.* **1990**, *59*, L31.

(69) Kanazirev, V.; Price, G. L.; Dooley, K. M. *Stud. Surf. Sci. Catal.* **1991**, *69*, 277.